Space-time ETAS models and an improved extension

Presenter
Akira Hikita (M1)

0. Outline

1. Introduction
2. Dvelopment of the ETAS model
3. Extension of the best fitted space-time model
4. Application to the data sets
5. Diagnosis analysis by stochastic declustering
6. Concluding remarks

1. Introduction

- Are seismic quiescence and activation the **precursors** to a large earthquake ?

Difficulty

- ➢ The quiescence is merely due to the reduction of aftershocks
- ➢ Too subjective

➡ We need to use a practical statistical space-time model that represents the ordinary seismic activity.

cf. the temporal ETAS model (Ogata, 1988)

2. Development of the ETAS model

Time only (Ogata, 1988)

$$\lambda_\theta(t) = \mu + \sum_{\{j:t_j<t\}} e^{\alpha\{M_j - M_c\}} \nu(t - t_j)$$

$$\ln L(\theta) = \sum_{i=1}^{N} \ln \nu(t_i) - \int_S^T \nu(t)\,\mathrm{d}t, \quad \theta = (K, c, p)$$

Space-time (Ogata, 1998)

$$\lambda_\theta(t,x,y) = \mu(x,y) + \sum_{\{j:t_j<t\}} \nu(t - t_j) \times g(x - x_j, y - y_j; M_j - M_c)$$

$$\ln L(\theta) = \sum_{i=1}^{N} \ln \lambda_\theta(t_i, x_i, y_i) - \int_S^T \iint_A \lambda_\theta(t,x,y)\,\mathrm{d}t\mathrm{d}x\mathrm{d}y$$

Ogata (1998)： 3 definitions of $g(x-x_j, y-y_j; M_j-M_c)$

$$g(x-x_j, y-y_j; M_j-M_c) = \exp\left[-\frac{1}{2}\frac{(x-x_j, y-y_j)\mathbf{S}_j(x-x_j, y-y_j)^t}{de^{\alpha(M_j-M_c)}}\right] \quad (5)$$

$$g(x-x_j, y-y_j; M_j-M_c) = \frac{e^{\alpha(M_j-M_c)}}{\left[(x-x_j, y-y_j)\mathbf{S}_j(x-x_j, y-y_j)^t + d\right]^q} \quad (6)$$

$$g(x-x_j, y-y_j; M_j-M_c) = \left[\frac{(x-x_j, y-y_j)\mathbf{S}_j(x-x_j, y-y_j)^t}{e^{\alpha(M_j-M_c)}} + d\right]^{-q} \quad (7)$$

$$v(t-t_j) = \frac{(p-1)c^{p-1}}{(t+c)^p}$$

Ogata (1998): Homogeneity and isotropy

Case 1. Homogeneous Poisson field for background seismicity and isotropic clustering

$$\mu(x, y) = \mu = constant, \qquad \boldsymbol{S} = 2 \times 2\ identity\ matrix$$

Case 2. Non-homogeneous Poisson field for background seismicity and isotropic clustering

$$\mu(x, y) = \nu\mu_0(x, y), \qquad \boldsymbol{S} = 2 \times 2\ identity\ matrix$$

Case 3. Non-(?)homogeneous Poisson field for background seismicity and anisotropic clustering (p. 16)

$$\mu(x, y) = \nu\mu_0(x, y), \quad \boldsymbol{S} = 2 \times 2 \text{ positive-define symmetric matrix}$$

Ogata (1998): Result

- The AIC always selected the g definition (7)

$$g(x - x_j, y - y_j; M_j - M_c) = \left[\frac{(x - x_j, y - y_j)\mathbf{S}_j(x - x_j, y - y_j)^t}{e^{\alpha(M_j - M_c)}} + d \right]^{-q} \quad (7)$$

  - Power law
  - The Utsu-Seki formula $\log_{10} A = M + 4.0$

    A : the area of the aftershock zone

    M: the magnitude

- Zuang et al. (2004) also shows that the (7) definition is best. However, the diagnosis analysis based on the stchastic declustering algorithm reveals **a significant bias in the spatial scaling factor.**

3. Extension of the best fitted space-time model

- The multiplication of time and space distribution

$$\kappa(M) \times \frac{(p-1)c^{p-1}}{(t+c)^{p}} \times \left[\frac{1}{\pi\sigma(M)} h\left\{\frac{(x,y)\boldsymbol{S}(x,y)^{t}}{\sigma(M)}\right\}\right] \quad (9)$$

In Ogata (1998), $\kappa(M) = \text{const.} \times \sigma(M) \propto e^{\alpha M}$

When the constraint is removed, the form (7) turns into

$$g(x-x_j, y-y_j; M_j - M_c) = e^{(\alpha-\gamma)(M_j - M_c)} \times \left[\frac{(x-x_j, y-y_j)\boldsymbol{S}_j(x-x_j, y-y_j)^{t}}{e^{\gamma(M_j - M_c)}} + d\right]^{-q} \quad (10)$$

3. Extension of the best fitted space-time model

$$g(x-x_j, y-y_j; M_j-M_c) = e^{(\alpha-\gamma)(M_j-M_c)} \times \left[\frac{(x-x_j, y-y_j)\boldsymbol{S}_j(x-x_j, y-y_j)^t}{e^{\gamma(M_j-M_c)}} + d\right]^{-q} \quad (10)$$

Zuang et al. (2004) implies that

$$\tilde{\gamma} = 0.50\log_e 10 \approx 1.15 \quad (11)$$

This agrees with the famous empirical formulae

$\log_{10}A = M + 4.0$ in Utsu and Seki (1955)

$\log_{10}L = 0.5\,M - 1.8$ in Utsu (1961)

M: magnitude

A : area of the aftershock zone

L : length of the aftershock zone

4. Application to the data sets

3 ways of definition of $g(x-x_j, y-y_j; M_j-M_c)$

- $$g(x-x_j, y-y_j; M_j-M_c) = \left[\frac{(x-x_j, y-y_j)\mathbf{S}_j(x-x_j, y-y_j)^t}{e^{\alpha(M_j-M_c)}} + d\right]^{-q} \qquad (7)$$

- $$g(x-x_j, y-y_j; M_j-M_c) = e^{(\alpha-\gamma)(M_j-M_c)} \times \left[\frac{(x-x_j, y-y_j)\mathbf{S}_j(x-x_j, y-y_j)^t}{e^{\gamma(M_j-M_c)}} + d\right]^{-q} \qquad (10)$$

- $\tilde{\gamma} = 0.50\log_e 10 \approx 1.15$ in (10) (11)

4. Application to the data sets

3 cases about homogeneity and isotropy

Case 1. Homogeneous Poisson field for background seismicity and isotropic clustering

$$\mu(x, y) = \mu = constant, \qquad \boldsymbol{S} = 2 \times 2 \; identity \; matrix$$

Case 2. Non-homogeneous Poisson field for background seismicity and isotropic clustering

$$\mu(x, y) = \nu\mu_0(x, y), \qquad \boldsymbol{S} = 2 \times 2 \; identity \; matrix$$

Case 3. Non-(?)homogeneous Poisson field for background seismicity and anisotropic clustering (p. 16)

$$\mu(x, y) = \nu\mu_0(x, y), \quad \boldsymbol{S} = 2 \times 2 \text{ positive-define symmetric matrix}$$

4. Application to the data sets

3 regions

The data in 1926-1995 compiled by JMA

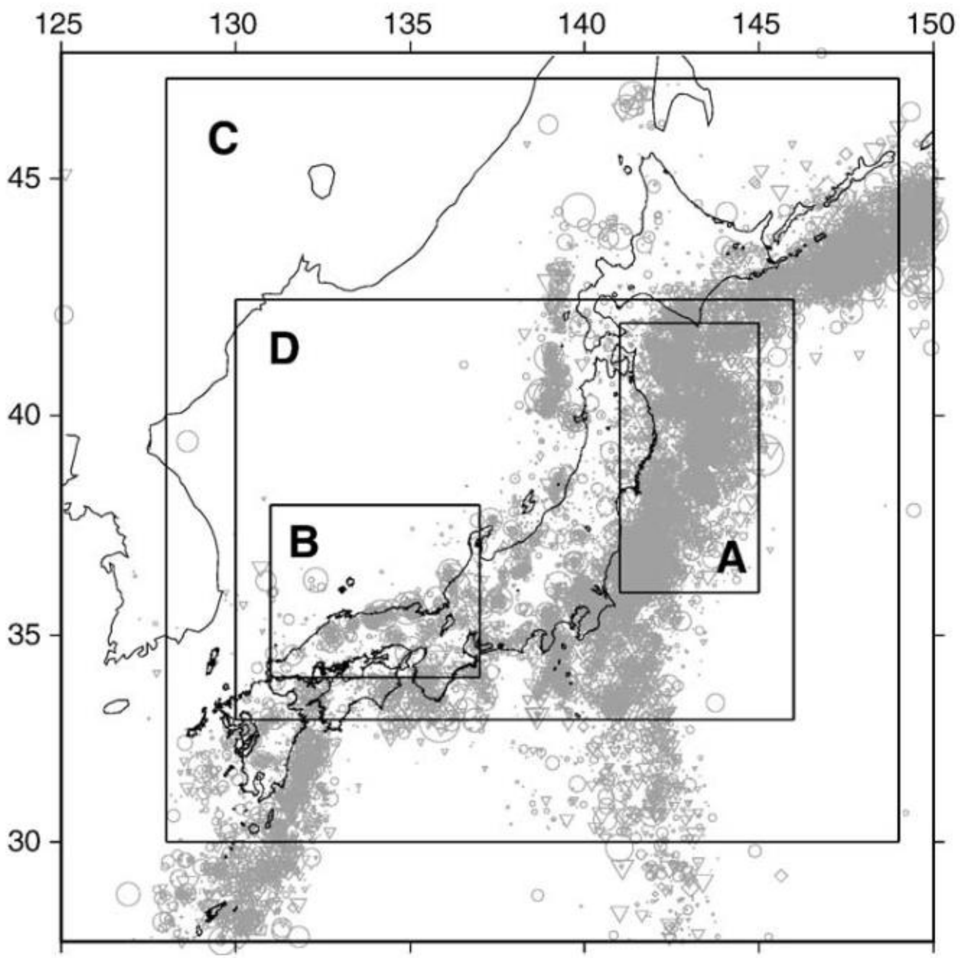

- **Region A**
  - Off the east coast of Tohoku
  - M 4.5 and larger
  - Depth down to 100 km
- **Region B**
  - Western part of Honshu Island
  - M 4.0 and larger
  - Depth down to 45 km
- **Region C**
  - In and around Japan
  - M 5.0 and larger
  - Depth down to 65 km

Result: AIC

		Case 1.	Case 2.	Case 3.
Region A	(7)	0.0	-1037.7	-1059.3
	(10)	0.6	-1057.6	-1081.4
	(11)	-0.6	-1053.3	-1077.6
Region B	(7)	0.0	-662.1	-678.6
	(10)	-3.2	-675.1	-693.8
	(11)	19.0	-653.8	-672.3
Region C	(7)	0.0	-1426.7	-1453.6
	(10)	-13.2	-1435.0	-1521.1
	(11)	-0.7	-1436.7	-1522.5

Result: p value

		Case 1.	Case 2.	Case 3.
Region A	(7)	0.909	1.043	1.043
	(10)	0.910	1.050	1.050
	(11)	0.910	1.053	1.043
Region B	(7)	0.961	1.027	1.027
	(10)	0.961	1.028	1.029
	(11)	0.960	1.027	1.028
Region C	(7)	0.910	1.021	1.020
	(10)	0.911	1.026	1.026
	(11)	0.910	1.026	1.026

$p < 1$ indicates that the assumption of **homogeneous background seismicity** is **inappropriate**

$$\kappa(M) \times \frac{(p-1)c^{p-1}}{(t+c)^p} \times \left[\frac{1}{\pi\sigma(M)} h\left\{\frac{(x,y)\boldsymbol{S}(x,y)^t}{\sigma(M)}\right\}\right] \quad (9)$$

Result: AIC

		Case 1.	Case 2.	Case 3.
Region A	(7)	0.0	-1037.7	-1059.3
	(10)	0.6	-1057.6	-1081.4
	(11)	-0.6	-1053.3	-1077.6
Region B	(7)	0.0	-662.1	-678.6
	(10)	-3.2	-675.1	-693.8
	(11)	19.0	-653.8	-672.3
Region C	(7)	0.0	-1426.7	-1453.6
	(10)	-13.2	-1435.0	-1521.1
	(11)	-0.7	-1436.7	-1522.5

- Both in Case 2. and Case 3., AIC in (10) is smaller than that in (7)
- The parameter values in Case 2. and Case 3. are similar
- AIC values in (10) and (11) are similar in Case 2. and Case 3.

Discussion

- The definition (10) improves the goodness-of-fit than (7)

$$g(x-x_j, y-y_j; M_j - M_c) = e^{(\alpha-\gamma)(M_j-M_c)} \times \left[\frac{(x-x_j, y-y_j)\boldsymbol{S}_j(x-x_j, y-y_j)^t}{e^{\gamma(M_j-M_c)}} + d \right]^{-q} \qquad \textbf{(10)}$$

- It is not very clear whether or not the anisotropic modeling improves the goodness-of-fit
- Reducing parameters may be possible by fixing γ in (11)

5. Diagnostic analysis by stochastic declustering

- Zuang et al. (2004)

The probability of the *j*-th event being a background event is

$$\phi_j = \mu(t_j, x_j, y_j) / \lambda(t_j, x_j, y_j)$$

The probability of the *j*-th event being triggered by the *i*-th event is

$$\rho_j = 1 - \phi_j = \Sigma_{\{i:\ i<j\}} \rho_{i,j}$$

$$\rho_{i,j} = \nu(t_j - t_i) g(x_j - x_i, y_j - y_i; M_i - M_c) / \lambda(t_j, x_j, y_j)$$

The stochastic declustering is understood to be a simuation, a bootstrap resampling

5. Diagnostic analysis by stochastic declustering

- Zuang et al. (2004)

In order to examine the approximation of the function form $\exp\{\alpha(M - M_c)\}/d$

Zuang et al. (2004) calculated the distances $r_{i,j}$

between a trrigered event j and its direct ancestor, event i

belong to a given magnitude band $M_i \in \Delta M$

$$\log L(D) = \sum_{\{i;\, M_i \in \Delta M\}} \sum_{\{j;\, i<j\}} \rho_{i,j} \log\left\{ \frac{2(q-1)D^{q-1} r_{i,j}}{\left(r_{i,j}^2 + D\right)^q} \right\}$$

(see Eggermont and LaRiccia (2001), section 2.4)

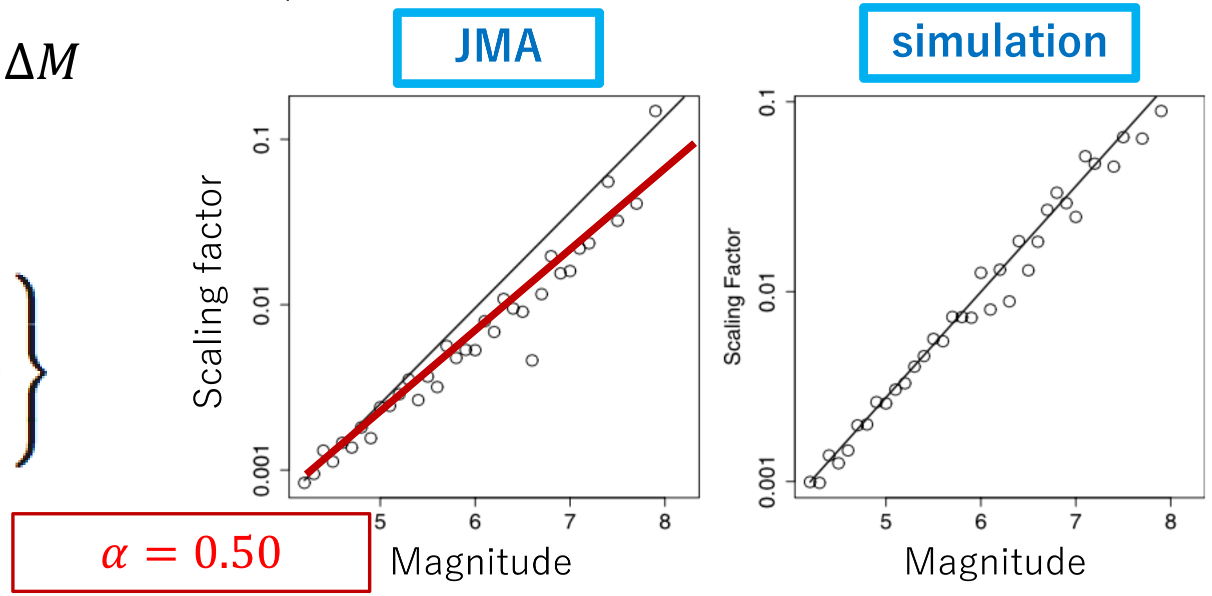

Figure 14. Reestimated D_M^2 for (a) the JMA catalogue and (b) the simulated catalogue. Theoretical fitting curves, $D^2 e^{\alpha(M-M_C)}$, are represented by the straight lines.

5. Diagnostic analysis by stochastic declustering

Result

✓ (7)

$\widehat{D}$ plot alignment has a smaller slope than that of the log-plot of $\hat{d}e^{\alpha(M-M_c)}$

✓ (10)

similar plot obtained by the model (10)

➡ The model with (10) has less bias than Zuang et al. (2004)

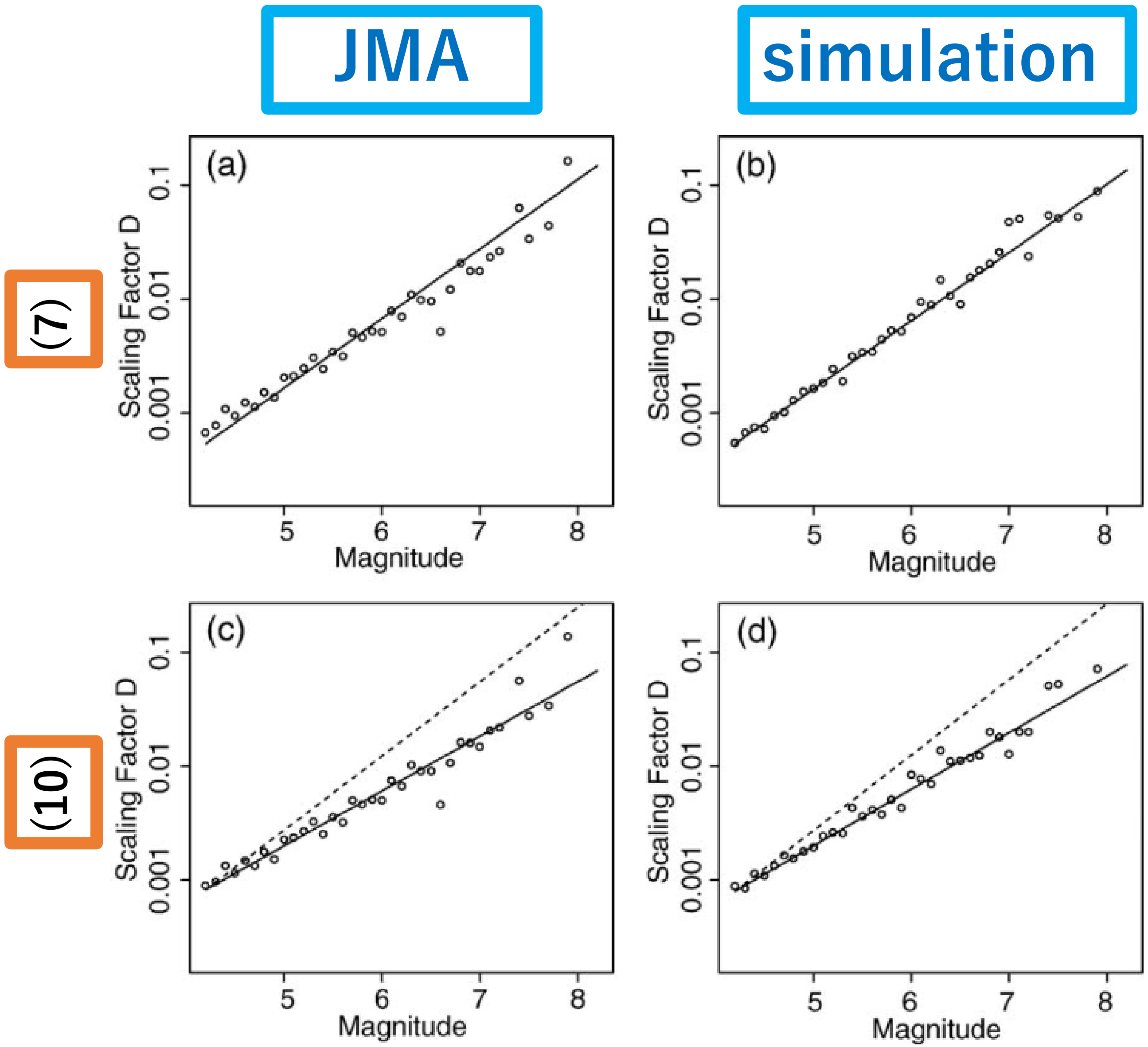

6. Concluding remarks

- We want to use earthquakes smaller than the minimum threshold magnitude

- However, the detected rate of the earthquakes in a catalogue changes both with location and with time

- Our next step is to develop the improved model, taking account of the space-time detection rate as a function of M, t, x, y